Chapter III

VISCOELASTIC BEHAVIOR OF PROTEIN HYDROGELS CROSS-LINKED BY CHEMICAL AND PHYSICAL NETWORK JUNCTIONS

1. Abstract

The primary sequences of proteins carry information that specifies intermolecular association and higher-order functions such as catalysis, cellular signaling, and the formation of tough, elastic materials. This chapter describes a set of recombinant artificial proteins that can be cross-linked by covalent bonds, by association of helical domains, or by both mechanisms. These proteins were used to construct molecular networks in which the mechanism of cross-linking determines whether the material response to mechanical deformation is elastic or viscoelastic. In viscoelastic networks, stress relaxation and energy dissipation can be tuned by controlling the ratio of physical cross-linking to chemical cross-linking, and the physical cross-links can be disrupted either by protein denaturation or by mutation of the primary sequence. This work demonstrates how protein sequence can be used to engineer the time-dependent responses of macromolecular networks to mechanical deformation.

Content from this chapter was published as: L.J. Dooling, M.E. Buck, W.-B. Zhang, and D.A. Tirrell. “Programming molecular association and viscoelastic behavior in protein networks.” *Advanced Materials*. doi:10.1002/adma.201506216

2. Introduction

Protein-based materials such as fibers, films, and gels derive many of their macroscopic properties from the folded structures and hierarchical assembly specified by the primary amino acid sequence. Despite important recent progress in the chemical synthesis of sequence-controlled polymers, biological synthesis remains the most powerful route to polymers of well-defined sequence and length [1]. Furthermore, although elucidation of the rules governing protein folding remains an important challenge, our understanding of the relationship between primary sequence and higher order structure is more advanced for proteins than for synthetic polymer systems [2]. For these reasons, recombinant artificial proteins constitute a promising class of macromolecules for engineering materials with macroscopic properties that are specified by the sequences of their constituent polymers.

Hydrogels are cross-linked polymeric or supramolecular networks that absorb large amounts of water. They are typically soft and highly swollen, characteristics that make them attractive materials for biomedical engineering applications such as tissue regeneration and cell culture [3, 4]. As discussed in Chapter 1, hydrogel networks can be prepared from artificial proteins by covalent cross-linking of side chain functional groups such as the ε-amine of lysine or the sulfhydryl of cysteine [5, 6]. Alternatively, networks can be cross-linked by noncovalent interactions among folded protein domains that assemble into higher-order structures such as coiled coils and triple helices [7, 8]. These two approaches produce chemical hydrogels and physical hydrogels, respectively. In both cases, the density of cross-linking sites and their location within the hydrogel backbone are specified by the sequence of the artificial protein. Together, the density and type of cross-linking determine the response of the hydrogel to macroscopic deformation. Covalent cross-links formed by irreversible chemical reactions maintain the shape

and elasticity of hydrogels and are essentially permanent. Physical cross-links are often transient, leading to stress relaxation, flow, and material erosion [9]. Encoding desired mechanical properties, material dynamics, and responsiveness to stimuli may require multiple types of cross-linking. The modular nature of genetically encoded artificial proteins is well-suited to this approach. To this end, this chapter describes the viscoelastic behavior of hydrogels prepared from artificial proteins that were designed to form chemical networks, physical networks, and chemical-physical networks.

3. Materials and Methods

3.1 Plasmid Construction

Genes encoding the artificial proteins used in this study were created using a combination of gene synthesis (Genscript, Piscataway, NJ) and standard molecular cloning techniques. The artificial protein PEP was encoded on the pET15b plasmid (pET15b PEP) (Novagen, Madison, WI). All other proteins were encoded on pQE-80L plasmids (pQE-80L EPE, pQE-80L ERE, pQE-80L EPE L44A) (Qiagen, Valencia, CA). The complete amino acid sequence for each protein is given in Appendix A.

3.2 Protein Expression and Purification

Chemically competent BL21 *Escherichia coli* (New England BioLabs, Ipswich, MA) were transformed with plasmids encoding the artificial proteins EPE, ERE, and EPE L44A. Expression was carried out at 37 °C in Terrific broth containing 100 μg mL^{-1} ampicillin (BioPioneer, San Diego, CA). At an optical density at 600 nm (OD_{600}) of 0.9-1, expression was induced with 1 mM isopropyl β-D-1-thiogalactopyranoside (IPTG) (BioPioneer). The cells were harvested 4 hr after

induction by centrifugation at 6000 *g*, 4 °C for 8 min. Cell pellets were subjected to two freeze-thaw cycles, resuspended in TEN buffer (10 mM Tris, 1 mM EDTA, 100 mM NaCl, pH 8.0) at a concentration of 0.5 g mL^{-1}, and subjected to a final freeze-thaw cycle. The lysate was treated with 10 μg mL^{-1} DNase I (Sigma, St. Louis, MO), 5 μg mL^{-1} RNase A (Sigma), 5 mM $MgCl_2$, and 1 mM phenylmethylsulfonyl fluoride (Gold Biotechnology, Olivette, MO) while shaking at 37 °C, 250 rpm for 30 min. Cell lysis was completed by sonication with a probe sonicator (QSonica, Newton, CT).

The artificial proteins were purified based on the inverse temperature transition associated with elastin-like polypeptides (ELPs). To prevent chain extension of the target proteins by disulfide formation, 0.1% (v/v) β-mercaptoethanol (β-ME) (Sigma) was added to the lysate. The lysate was cooled to 4 °C and clarified by centrifugation at 39,000 *g*, 4 °C for 1 hr. To depress the lower critical solution temperature of the hydrophilic ELPs, sodium chloride was added to the supernatant to a final concentration of 2 M. After shaking at 37 °C for 1 hr, aggregated proteins were pelleted by centrifugation at 39,000 *g*, 37 °C for 1 hr. The target proteins were extracted from the pellet with water containing 0.1% (v/v) β-ME overnight at 4 °C. This process was repeated twice but the β-ME was omitted. Instead, after the second and third temperature cycles, the proteins were reduced with 5 mM tris(hydroxypropyl)phosphine (THP) (Santa Cruz Biotechnology, Dallas, TX) at 4 °C. Residual salt and reducing agents were removed by desalting using Zeba 7K MWCO columns (Thermo Fisher Scientific, Waltham, MA) equilibrated with degassed distilled and deionized water (ddH_2O). The proteins were lyophilized and stored under argon at -80 °C. Typical yields of EPE and ERE were 200 mg L^{-1} and 100 mg L^{-1} of culture, respectively.

Expression of PEP from the pET15b plasmid requires the BL21(DE3) *E. coli* strain (Novagen) containing the T7 RNA polymerase. Protein expression was performed in Terrific broth

containing 100 μg mL^{-1} ampicillin. Cells were grown at 37 °C until the OD_{600} reached 0.9-1.0. Protein expression was induced with the addition of 1 mM IPTG and proceeded for 5 hr, after which time the cells were harvested and lysed with 8 M urea. Cells suspended in 8 M urea were subjected to three freeze/thaw cycles followed by sonication. Clarified lysates were obtained by centrifugation and PEP was isolated by affinity chromatography with nickel nitriloacetic acid (NiNTA) resin (Qiagen) under denaturing conditions. The elution fractions containing purified PEP were combined, dialyzed against distilled water for 48 hr at 4 °C using a MWCO 12,000-14,000 membrane (Spectrum Laboratories, Rancho Dominquez, CA), and lyophilized. Yields of PEP were approximately 100 mg per liter of culture.

3.3 MALDI-TOF Mass Spectrometry

Lyophilized proteins (EPE, ERE, EPE L44A, and PEP) were dissolved in ddH_2O at a concentration of 10 mg mL^{-1}. The protein solutions were mixed with sinapinic acid matrix (10 mg mL^{-1} in 6:3:1 water:acetonitrile:1% trifluoroacetic acid) at volumetric ratios varying from 4:1 to 10:1 (matrix to protein). The mixtures were spotted on the MALDI sample plate and allowed to dry. Spectra were acquired on a Voyager DE Pro spectrometer (Applied Biosystems, Carlsbad, CA).

3.4 Measurement of Protein Thiol Content by Ellman's Assay

Ellman's reagent, 5,5'-dithio-bis-(2-nitrobenzoic acid), (Sigma) was used to measure the concentration of free thiols as described in Chapter 2. Briefly, protein was dissolved at a concentration of 5 mg mL^{-1} in reaction buffer (100 mM sodium phosphate, 1 mM EDTA, pH 8.0). In a cuvette, the protein solution (125 μL) and Ellmans' reagent (50 μL, 5 mg mL^{-1} in reaction

buffer) were added to the reaction buffer (2.5 mL). The reaction was incubated for 15 min and the absorbance at 412 nm was measured on a Cary 50 UV/VIS spectrophotometer (Varian, Palo Alto, CA). The thiol concentration was calculated using the molar extinction coefficient 14,150 M^{-1} cm^{-1} [2].

3.5 Hydrogel Preparation

To prepare EPE, ERE, and EPE L44A hydrogels, lyophilized protein was resuspended in degassed 100 mM sodium phosphate, 6 M guanidinium chloride, 400 mM triethanolamine (Sigma) at a concentration of 150 mg mL^{-1}. The 4-arm, 10 kDa PEG vinyl sulfone cross-linker (JenKem Technology USA, Plano, TX) was dissolved in degassed 400 mM triethanolamine at a concentration of 150 mg mL^{-1}. To facilitate dissolution, samples were sonicated in an ultrasonic bath for 1 min and centrifuged at 10,000 *g* for 1 min. The pH of the protein and cross-linker solutions was adjusted to approximately 7.2-7.4 using 6 N HCl. The cross-linker was added to the protein solution at a volumetric ratio that gave a nominal 1:1 thiol to vinyl sulfone stoichiometry. However, based on the thiol quantification using Ellman's assay, the vinyl sulfone was in approximately 1.2-fold excess. After vortexing to mix, a droplet (40 μL) was pipetted onto a glass slide that had been treated with SigmaCote siliconizing fluid (Sigma). The droplet was flattened into a disk by placement of another treated glass slide separated by 0.5 mm silicone spacers (McMaster-Carr, Santa Fe Springs, CA), and the slides were clamped tightly. Gelation occurred within several minutes, but hydrogels were cured overnight (>12 hr) in the dark. The cross-linked hydrogels were swollen in decreasing concentrations of guanidinium chloride (6 M, 3 M, 2 M, 1 M for 3 hr each) in phosphate-buffered saline (PBS) (1.5 mM KH_2PO_4, 4.3 mM Na_2HPO_4, 137 mM NaCl, 2.7 mM KCl, pH 7.4) to remove any unreacted material. The gels were then swollen in

PBS containing 0.02% (w/v) sodium azide (to inhibit microbial growth during swelling) for at least 48 hr.

PEP hydrogels were formed by suspending lyophilized protein in PBS containing 0.02% (w/v) sodium azide. The solutions were placed on ice for 2-4 hr or until a clear solution was formed. The gels were centrifuged briefly to remove all air bubbles. For experiments assessing the denaturing effects of urea on PEP hydrogels, lyophilized protein was suspended in solutions of increasing concentration of urea dissolved in 100 mM sodium phosphate buffer. The pH of each solution was adjusted to 7.4 and the final protein concentration was 7% (w/v).

3.6 Rheological Characterization of Protein Hydrogels

Rheological experiments with ERE, EPE, and mixed composition hydrogels were performed on an ARES-RFS strain-controlled rheometer (TA Instruments, New Castle, DE) equipped with an 8 mm parallel plate test geometry. Swollen hydrogels were cut to this size using an 8 mm biopsy punch (Miltex, York, PA). The gap height was set by lowering the geometry until a plateau in the storage modulus (measured at 5 rad s^{-1} and 1% strain) was reached as described previously [10]. The edge of the gel was surrounded with paraffin oil to minimize evaporation. Strain sweep experiments from 0.01-10% strain amplitude were performed at 5 rad s^{-1} to determine the linear viscoelastic region. Frequency sweep experiments from 100 to 0.001 rad s^{-1} were performed at 1% strain amplitude. The temperature was maintained at 25 °C by a Peltier thermoelectric device. Following frequency sweep experiments, stress relaxation experiments were also performed under 1% strain for 2 hr. For PEP gels, the ARES-RFS was equipped with a 25 mm diameter cone and plate geometry (0.04 rad cone angle). For PEP in 8 M urea, frequency sweep experiments were performed at 10% strain amplitude.

3.7 Swelling Measurements

Swollen hydrogels were blotted with filter paper to remove excess buffer, weighed on an analytical balance (Mettler Toledo, Columbus, OH) to obtain the swollen mass, and placed in ddH_2O for 48 hr with several changes to remove salts. They were then transferred to microcentrifuge tubes, frozen with liquid nitrogen, and lyophilized to obtain the dry mass. The mass swelling ratio, Q_m, is equal to the swollen mass divided by the dry mass. The same procedure was followed for EPE and ERE gels swollen in PBS containing 8 M urea.

4. Results and Discussion

4.1 Protein Design, Synthesis, and Characterization

The artificial proteins EPE and ERE designed for this study feature a triblock architecture in which the endblocks are elastin-like polypeptides (ELPs) containing repeats of the pentapeptide VPGXG (Figure III-1a, see Appendix A for full sequences). The guest position X is occupied by either valine or glutamic acid (at a ratio of 4:1 Val:Glu). This composition was selected to raise the lower critical solution temperature of the elastin-like domains sufficiently that these domains would remain soluble at the temperatures and ionic strengths of interest [11]. Cysteines at the protein termini were included as sites for covalent cross-linking. The midblock domain P of EPE is derived from the N-terminal fragment of the rat cartilage oligomeric matrix protein (COMP). This domain forms homopentameric coiled coils and is responsible for oligomerization of native COMP [12]. ERE also features ELP endblocks and terminal cysteine residues, but in place of the coiled-coil midblock it contains a 17-amino acid sequence (denoted R) derived from the integrin-binding loop of fibronectin [13]. This sequence contains the RGD (Arg-Gly-Asp) tripeptide widely used in cell adhesion studies, but it is not expected to contribute significant interchain interactions.

The EPE and ERE proteins have molar masses of 21.5 and 18.5 kg mol^{-1}, respectively. This difference is expected to have only a small effect on the mechanical properties of materials prepared from these proteins. Much more significant effects are expected to arise from the capacity of the P domain, but not R, to associate and form non-covalent network junctions.

The EPE and ERE proteins were expressed in *Escherichia coli* strain BL21 and purified by inverse temperature cycling [14]. Purity and molecular weight were assessed by SDS-PAGE (sodium dodecyl sulfate polyacrylamide gel electrophoresis) and MALDI-TOF (matrix-assisted laser desorption/ionization time-of-flight) mass spectrometry (Figures III-2 and III-3). After reduction with tris(hydroxypropyl)phosphine, desalting, and lyophilization, the free thiol content of each protein was measured using Ellman's assay (Figure III-4 a). While the proteins are shown to be monomeric by non-reducing SDS-PAGE (Figure III-4 b and c), approximately 15-20% appear to form a cyclic product through an intramolecular disulfide bond between the N- and C-terminal cysteines.

A third protein, denoted PEP, was also designed with a sequence that is similar to ERE but contains P endblocks in place of the terminal cysteine residues (Figure III-1a). PEP was expressed in the BL21(DE3) strain of *E. coli* and purified by immobilized metal affinity chromatography using nickel nitriloacetic acid agarose resin.

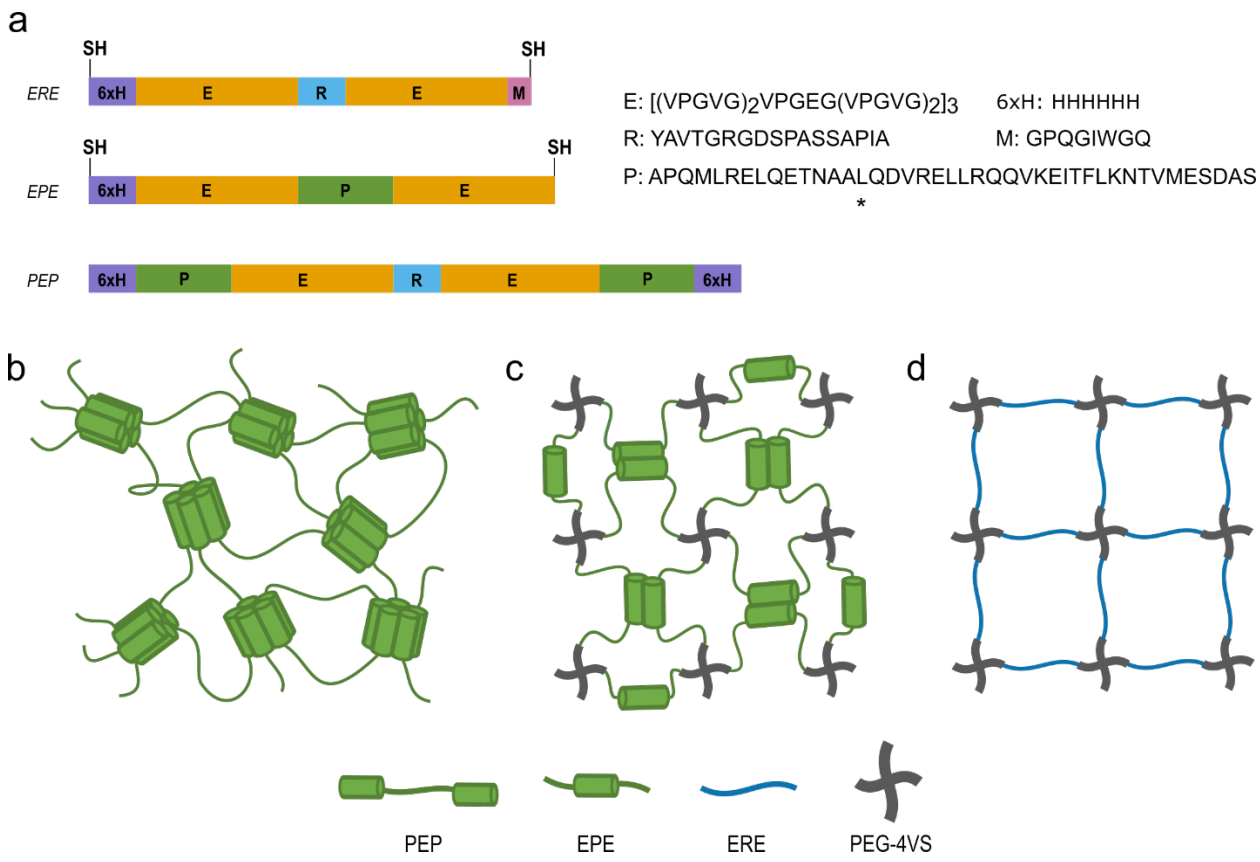

Figure III-1. Artificial protein design and cross-linking scheme. (**a**) Artificial proteins EPE and ERE consist of terminal cysteine residues (-SH), elastin-like endblocks E, and either the P or R midblock domain. ERE also contains an octapeptide recognition sequence M for proteolytic cleavage. The artificial protein PEP contains two P domains near the termini that flank the elastin-RGD-elastin sequence. The * below the sequence of the P domain denotes the position of leucine 44, which was mutated to alanine to create the variant EPE L44A. (**b**) PEP forms physical hydrogels through association of the P endblocks. (**c**) EPE and (**d**) ERE require covalent cross-linking with 4-arm PEG vinyl sulfone to form gels. ERE contains only covalent cross-links while EPE also has the potential to form physical cross-links through association of the midblock domains. Although P assembles in pentameric coiled coils in COMP, the physical cross-links are depicted as dimers in (c) for clarity.

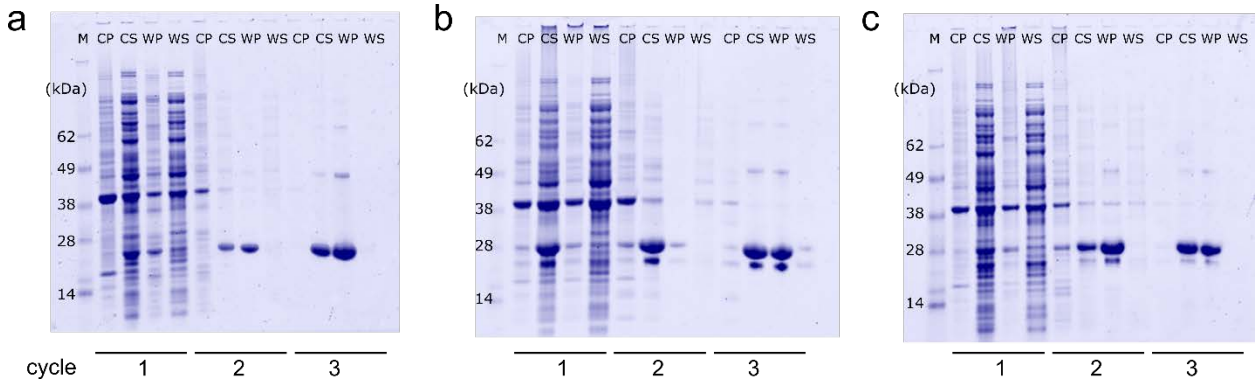

Figure III-2. SDS-PAGE of artificial proteins during inverse temperature cycling. ERE (**a**), EPE (**b**), and EPE L44A (**c**) were purified by three cycles of inverse temperature cycling. After each centrifugation step, samples of the supernatant and pelleted fractions were saved. The target proteins are expected to be soluble in the cold step (4 °C, low ionic strength) and insoluble in the warm step (37 °C, 2 M NaCl). For SDS-PAGE analysis, the proteins in the pelleted fractions were extracted in 8 M urea. The samples were boiled in SDS loading buffer with 2.5% (v/v) β-ME to reduce disulfide bonds. The gel was stained with colloidal blue stain to visualize proteins. After 3 cycles of cold and warm spins, the target proteins were successfully purified from the *E. Coli* lysates. (Abbreviations: CP – cold pellet, CS – cold supernantant, WP – warm pellet, WS – warm supernatant, M – SeeBlue protein marker with molecular weights in kDa).

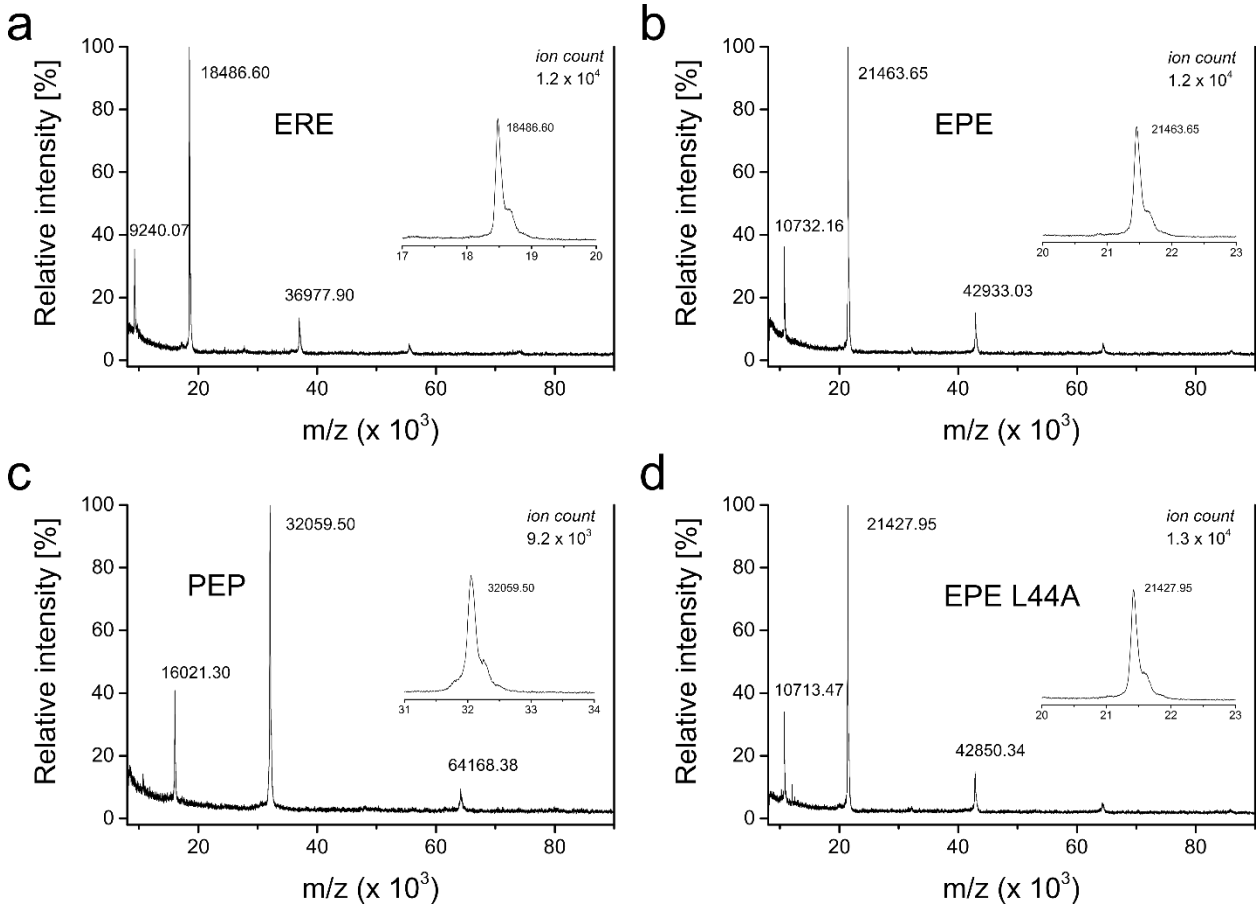

Figure III-3. MALDI-TOF mass spectrometry of purified artificial proteins. (**a**) ERE (calculated 18474, observed 18487), (**b**) EPE (calculated 21465, observed 21464), (**c**) PEP (calculated 32047, observed 32060), and (**d**) EPE L44A (calculated 21422, observed 21428). Peaks assigned to the doubly charged species and dimers are also labeled.

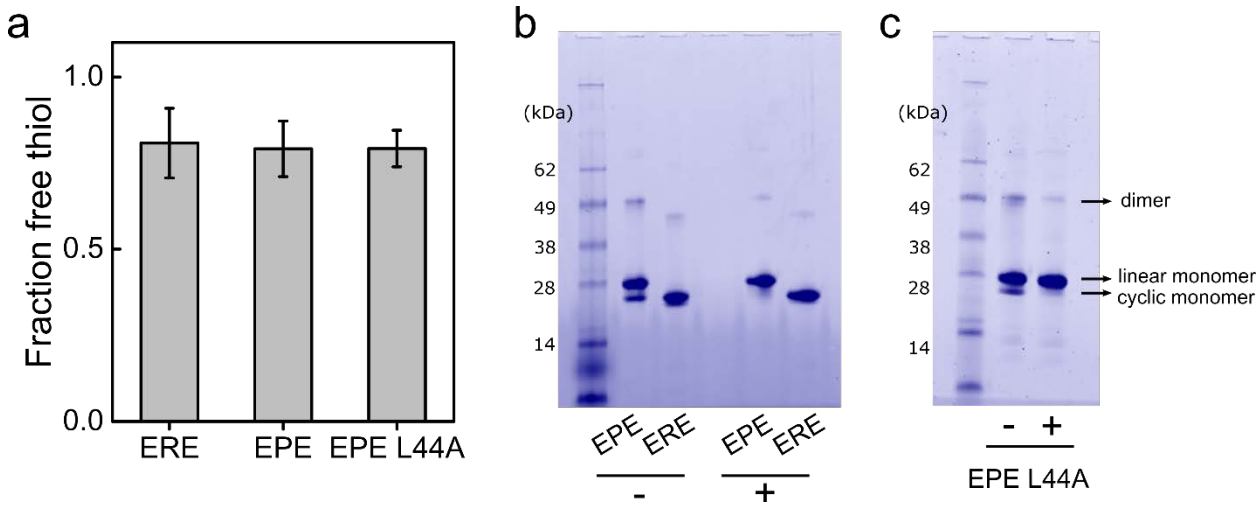

Figure III-4. Ellman's assay and non-reducing SDS-PAGE for purified artificial proteins. (**a**) Ellman's assay measures the concentration of free thiols in the protein preparations (*n* = 3, avg ± sd). The measured thiol concentration for each protein is approximately 80% of the expected concentration based on the amount of protein per reaction and assuming two cysteines per protein. SDS-PAGE performed on samples without reducing agent demonstrates that EPE, ERE (**b**) and EPE L44A (**c**) are primarily monomeric after desalting and lyophilization. However, approximately 20% of the monomeric protein is cyclized, consistent with the results of Ellman's assay in (a). The cyclized proteins run at a lower apparent molecular weight than the linear proteins and are absent in control lanes containing samples that were boiled in loading buffer containing 2.5% (v/v) β-ME as a disulfide reductant.

4.2 Hydrogel Cross-linking

Telechelic artificial proteins such as PEP and others that contain P domains at the N- and C-termini self-assemble into physical hydrogels through association of their endblocks (Figure III-1 b) [9, 15]. Hydrogels were formed from PEP by resuspending lyophilzed protein in PBS at 7 wt% for several hours on ice. Because each EPE protein chain contains only a single P domain, self-assembly of this protein into an extended hydrogel network is not possible, except perhaps under conditions that yield significant chain extension through disulfide bond formation [16]. However, EPE could still be incorporated into covalent hydrogel networks by cross-linking the terminal cysteine residues with 4-arm poly(ethylene glycol) vinyl sulfone (PEG-4VS) [17]. This cross-linking reaction was performed in buffer containing 6 M guanidinium chloride to prevent premature association of the P midblock domains. Swelling the resulting hydrogels in phosphate buffered saline to remove the denaturant allows the P domains within neighboring chains of the chemical network to associate and form physical cross-links (Figure III-1 c). Hydrogels were also prepared from ERE using the same method. Because ERE lacks the associative midblock domain found in EPE, these hydrogels are expected to exhibit only the properties of chemically cross-linked networks (Figure III-1 d). Together, these three artificial proteins demonstrate how a small set of sequences can be combined in different ways to yield chemical gels (ERE), physical gels (PEP), and chemical-physical gels (EPE).

4.3 Viscoelastic Behavior of ERE, EPE, and PEP Hydrogels

The three types of networks depicted in Figure III-1 b, c, and d are expected to exhibit different responses to material deformation. While the covalent cross-links in EPE and ERE gels are expected to be permanent because of the irreversibility of the thioether bond, the association

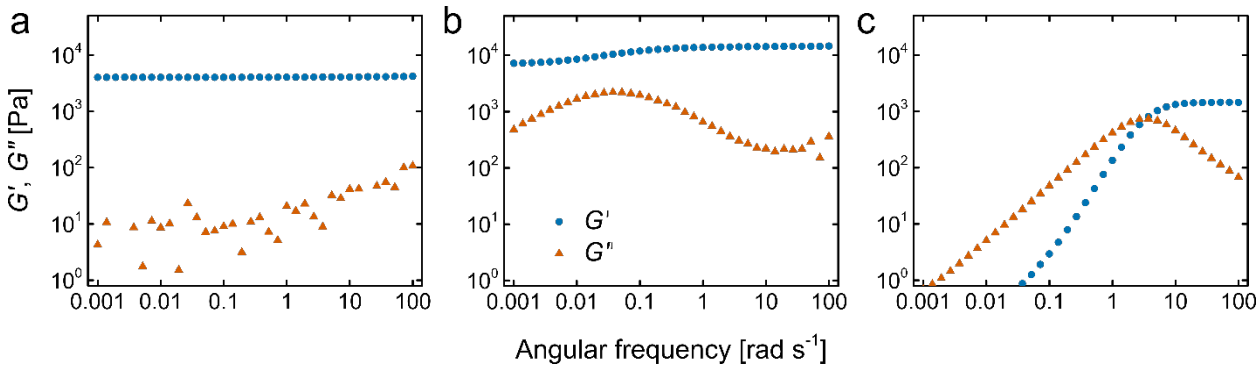

Figure III-5. Linear rheology of protein hydrogels. Small amplitude oscillatory shear rheology frequency sweeps for swollen ERE (**a**) and EPE (**b**) hydrogels at 1% strain amplitude, 25 °C. The mass swelling ratios for ERE and EPE are 19.7 and 13.5, respectively. Hydrogels prepared from EPE demonstrate a transition from a high frequency plateau to a low frequency plateau in *G'* as well as a local maximum in *G"* that coincides with this transition. This is attributed to the combination of permanent chemical cross-links and transient physical cross-links. These features are not observed in hydrogels prepared from ERE, which contain only chemical cross-links. In hydrogels prepared from PEP (**c**), only physical cross-linking is present and *G'* and *G"* exhibit a cross-over point at $\omega = 3.9$ rad s^{-1} (7 wt% protein, 1% strain amplitude, 25 °C).

of P domains in EPE and PEP gels is reversible, and the physical cross-links are expected to be transient. The transient nature of the association should allow stress stored in deformed chains to relax on timescales comparable to the lifetimes of the physical cross-links. To determine whether such relaxation occurs in PEP, EPE, or ERE hydrogels, we performed small amplitude oscillatory shear rheology experiments to measure the storage modulus (*G'*) and loss modulus (*G"*) of each gel over an angular frequency range of 0.001-100 rad s^{-1}. The storage modulus of hydrogels composed entirely of ERE is nearly independent of frequency, as expected for an elastic network connected entirely by covalent cross-links with few network defects (Figure III-5 a). In contrast, hydrogels prepared from EPE are viscoelastic and display a frequency-dependent storage modulus with both high and low frequency plateaus (Figure III-5 b). The high frequency plateau modulus,

denoted $G'(\infty)$, reflects the combined contributions of covalent and physical cross-linking. As the oscillation frequency is decreased, the timescale on which the gel is deformed becomes comparable to the characteristic timescale for exchange or dissociation of the physical cross-linking domains. This results in relaxation of some of the stress stored within the network. At very low frequencies or long times, the physical cross-links are no longer elastically effective but stress is still borne by the deformation of chains connected by covalent cross-links. For this reason, the low frequency storage modulus, $G'(0)$, is associated with the permanent chemical network.

PEP gels also exhibit high frequency plateau storage moduli, $G'(\infty)$, due to physical cross-linking between P domains (Figure III-5 c). Unlike EPE gels, however, PEP hydrogels lack chemical cross-links and exhibit a crossover point ($G' = G''$) corresponding to a transition between regimes of solid-like behavior ($G' > G''$) and liquid-like behavior ($G'' > G'$). This behavior is characteristic of viscoelastic fluids. In EPE hydrogels, which can be characterized as viscoelastic solids, no crossover is observed and $G' > G''$ for all frequencies measured. The loss moduli of EPE and PEP gels are both characterized by local maxima. In PEP, the maximum in G'' occurs near the crossover point. In EPE hydrogels, the maximum in G'' occurs as G' transitions between the high and low frequency plateaus. In contrast, no local maximum in G'' is observed in ERE gels, and accurate measurement of G'' is difficult because of uncertainty in determination of the phase angle in materials that do not dissipate significant amounts of energy. The relaxation time for the physical cross-links, which is determined from the frequency at which the maximum in G'' occurs, differs by nearly two orders of magnitude for PEP and EPE gels. This difference likely represents the effect of constraining the associative domain within a chemical network. A similar effect was observed in physical protein hydrogels cross-linked by P that also contained

entanglements introduced by oxidative chain extension, although the increase in the relaxation time was only 2-3 fold in these materials [16].

4.4 Viscoelastic Behavior of Hydrogels Prepared from Mixtures of EPE and ERE

In order to tune the properties of chemical-physical protein hydrogels, mixtures of EPE and ERE were cross-linked with PEG-4VS. Mixed composition hydrogels were prepared by cross-linking gel precursor solutions containing 75:25, 50:50, or 25:75 ERE:EPE by weight while maintaining the total protein concentration at 15 wt%. The resulting hydrogels behave as viscoelastic solids, but exhibit smaller ratios of $G'(\infty)$ to $G'(0)$ than those observed in EPE gels (Figure III-6 a). For EPE hydrogels, the ratio of $G'(\infty)$ to $G'(0)$ is approximately two as expected from the protein sequence; association of the P domains cuts the average molecular weight between cross-links in half. As the fraction of EPE in the gel is decreased, there are fewer chains that are capable of forming physical cross-links, and the smaller fraction of transient cross-links results in less stress relaxation. This effect is also evident in the behavior of G'', in which the maximum amplitude of the peak associated with stress relaxation diminishes as the fraction of EPE is decreased (Figure III-6 b). Despite ERE and EPE having similar molecular weights and identical covalent cross-linking sites, the storage moduli of the five gel preparations vary slightly even at low frequencies where physical cross-links are not expected to be elastically effective. This observation is consistent with the difference in the swelling ratios (or chain densities) of the networks (Figure III-6 d). Networks that contain more physical cross-linking are less swollen (denser) and therefore remain stiffer even at low frequencies. These results provide further evidence that physical cross-linking through the P domains is responsible for the time-dependent mechanical properties of networks containing EPE, and illustrate the potential for tuning the

viscoelastic and swelling behavior of protein hydrogels by controlling the ratio of physical and chemical cross-links.

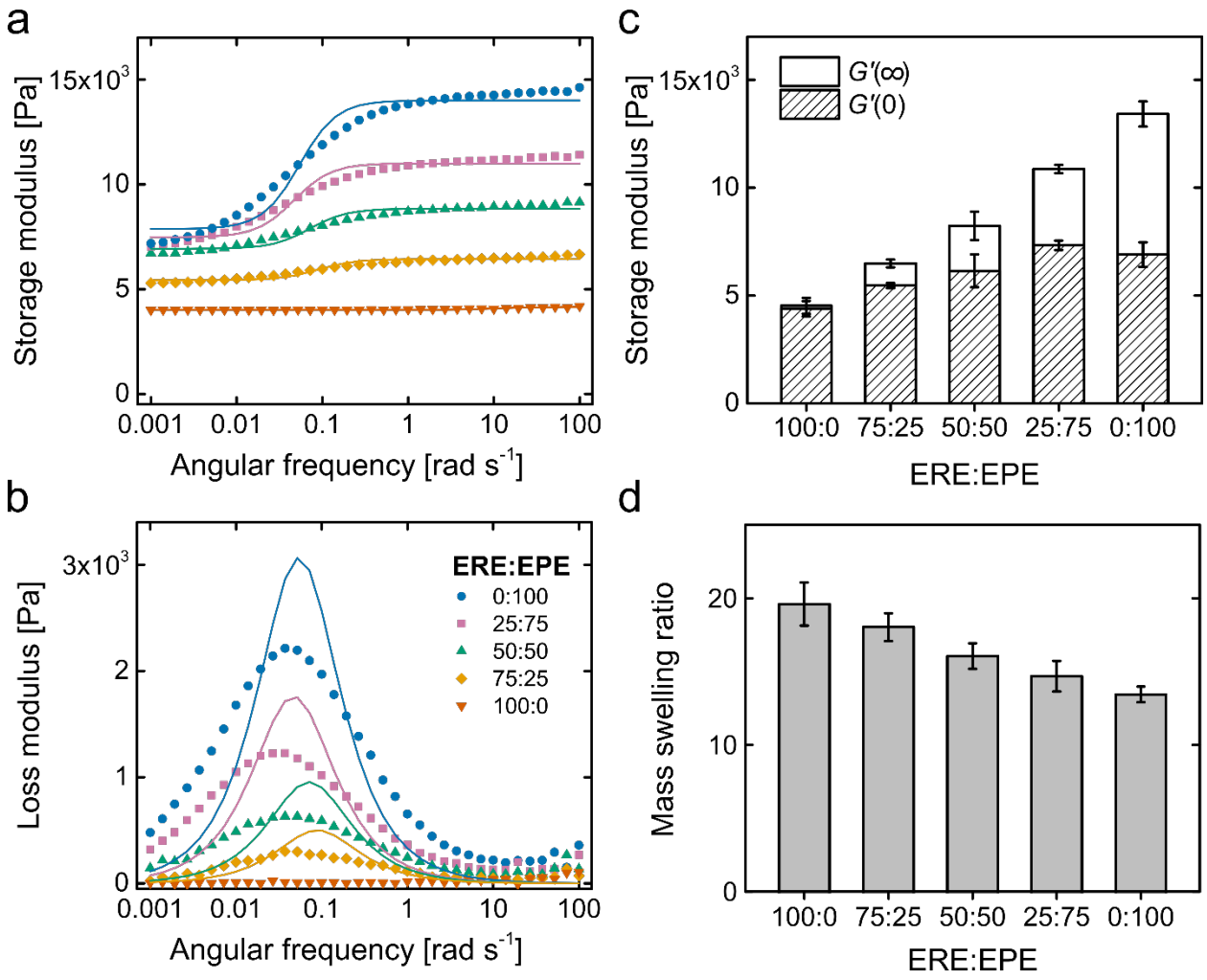

Figure III-6. Rheology and swelling of ERE:EPE chemical-physical hydrogels. Representative frequency sweep rheology showing the storage (**a**) and loss (**b**) moduli at 1% strain amplitude, 25 °C for hydrogels prepared from mixtures of EPE and ERE. The solid lines represent fits of the Maxwell expression for a viscoelastic solid (Equations III-1 and III-2) (**c**) The values of the plateau moduli $G'(\infty)$ and $G'(0)$ were acquired from fits of G' to the Maxwell model for a viscoelastic solid ($n \geq 3$, avg ± sd). The ratio of $G'(\infty)$ to $G'(0)$ and the maximum in G'' increase as the fraction of EPE is increased. (**d**) The mass swelling ratio Q_m of the ERE:EPE hydrogels decreases as the fraction of EPE is increased (n = 5, avg ± sd).

4.5 Rheological Models of Viscoelastic Protein Networks

The Maxwell expression for the storage modulus of a viscoelastic solid (Equations III-1) was used to fit the experimental values of $G'(\omega)$ for each ERE:EPE gel preparation.

$$G'(\omega) = G_0 + G\frac{(\omega\tau)^2}{1+(\omega\tau)^2} \qquad \text{(Equation III-1)}$$

$$G'' = G\frac{(\omega\tau)}{1+(\omega\tau)^2} \qquad \text{(Equation III-2)}$$

In the Maxwell expression, G_0 is the component of the storage modulus that is independent of the oscillation frequency, G describes the component of the storage modulus that varies with the oscillation frequency, and τ is the characteristic relaxation time [18, 19]. The parameters obtained from fitting the experimental $G'(\omega)$ (Table III-1) were used to evaluate the plateau moduli $G'(\infty)$ and $G'(0)$ plotted in Figure III-6 c. In the high frequency limit, the plateau storage modulus $G'(\infty)$ is equal to $G_0 + G$. In the low frequency limit, the plateau storage modulus $G'(0) = G_0$. The values G and τ determined by fitting the storage modulus to Eq. III-1 were also used to evaluate the loss modulus by Eq. III-2. The Maxwell model is only an approximation for the frequency-dependent behavior of ERE:EPE gels. The relaxations observed in the experimental data are broader than those predicted for a single Maxwell mode. Such broad relaxations in physical protein gels were observed by Tang *et al.* and were better fit with a stretched exponential model [16], which is discussed below. However, this analysis still provides a useful method to quantify the plateau values and relaxation times in the dynamic storage moduli.

Composition (ERE:EPE)	G (Pa)	G_0 (Pa)	τ (sec/rad)
100:0	135 ± 16	4391 ± 360	0.11 ± 0.02
75:25	1023 ± 64	5467 ± 120	10.6 ± 1.4
50:50	2087 ± 217	6144 ± 765	15.1 ± 1.0
25:75	3528 ± 25	7334 ± 217	23.8 ± 2.2
0:100	6517 ± 390	6901 ± 572	18.7 ± 0.8

Table III-1. Maxwell model parameters for ERE:EPE hydrogels. The experimental data were fit to Eq. III-1 to obtain the parameters G, G_0, and τ. These parameters were then used to generate the solid curves shown in Figure III-6 a and b and to evaluate the plateau moduli $G'(\infty)$ and $G'(0)$ in Figure III-6 c.

Relaxation in chemical-physical gels was also observed by measuring the stress in gels held at constant 1% strain for 2 hours (Figures III-7 and III-8). For stress relaxation experiments, the relaxation function, $G(t)$, was fit to a single exponential model,

$$G(t) = G\exp\left(-\frac{t}{\tau}\right) + G_e \qquad \text{(Equation III-3)},$$

a double exponential model,

$$G(t) = G_1\exp\left(-\frac{t}{\tau_1}\right) + G_2\exp\left(-\frac{t}{\tau_2}\right) + G_e \qquad \text{(Equation III-4)},$$

and a stretched exponential (or Kohlrausch-Williams-Watts, KWW) model [16],

$$G(t) = G\exp\left(-\left(\frac{t}{\tau_{KWW}}\right)^{\beta}\right) + G_e \qquad \text{(Equation III-5)}.$$

The parameter G_e in Eqs. III-3, III-4, and III-5 is the equilibrium modulus and is analogous to the low frequency modulus in the frequency sweep experiments. In the stretched exponential model, the exponent β reflects heterogeneity in the relaxation process and varies between 0 and 1, with β

= 1 reducing to the single exponential model given by Eq. III-3. The mean relaxation time, $\langle\tau\rangle$, is calculated as

$$\langle\tau\rangle = \frac{\tau_{KWW}}{\beta}\Gamma\left(\beta^{-1}\right) \qquad \text{(Equation III-6)}$$

where $\Gamma(\beta^{-1})$ is the gamma function evaluated at β^{-1}. As in the frequency sweep experiments, a single Maxwell element is not sufficient to fit the broadness of the relaxation. For this reason, the stretched exponential model was used to quantify stress relaxation in EPE and mixed composition hydrogels (Figure III-8 and Table III-2). Potential sources of hetergeneity that may broaden the relaxation include local variation in the chemical cross-linking density and deviation of the physical cross-linking aggreagation number from the expected value of 5.

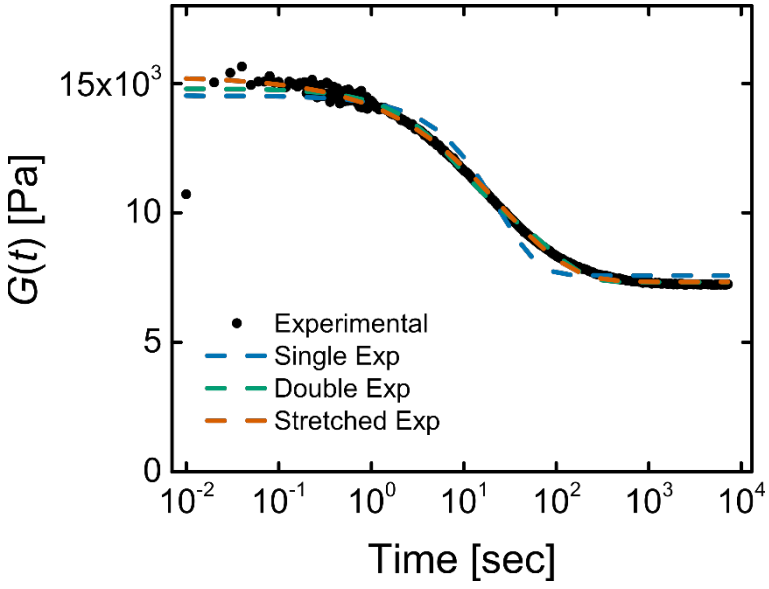

Figure III-7. Relaxation function for an EPE hydrogel fit to single exponential, double exponential, and stretched exponential models. The relaxation function $G(t)$ is plotted against time for a 1% strain over the duration of 2 hours. The dashed lines are fits of the experimental data to a single exponential model (Eq. III-3, blue), a double exponential model (Eq. III-4, green) and a stretched exponential model (Eq. III-5, orange). All of the models capture the short and long time plateau behavior, but the single exponential model does not fit the broadness of the relaxation.

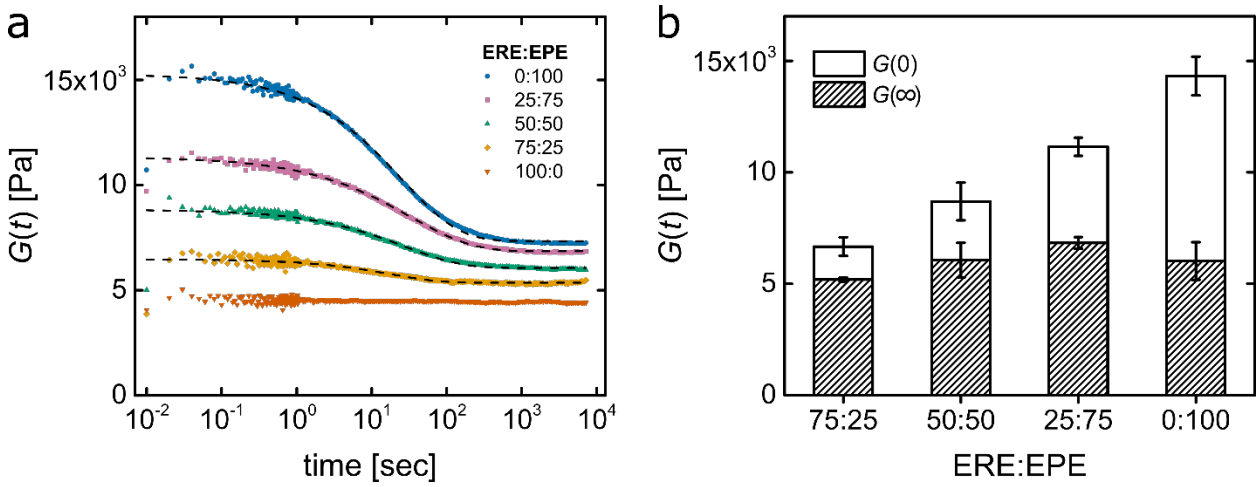

Figure III-8. Stress relaxation in ERE:EPE hydrogels. (**a**) Representative stress relaxation curves are shown for hydrogels prepared from EPE, ERE, and mixtures of the two proteins. The relaxation function $G(t)$ is plotted against time for a 1% strain over the duration of 2 hours. The dashed lines are fits of the experimental data to the stretched exponential model given in Eq. III-5. (**b**) The stretched exponential fit was evaluated at the limits $t = 0$ and $t \rightarrow \infty$ to give $G(0)$ and $G(\infty)$, respectively ($n \geq 3$, avg ± sd). The relaxation function at these limits is in agreement with $G'(\infty)$ and $G'(0)$ from the frequency sweep experiments. The ERE hydrogel does not exhibit significant stress relaxation and was not fit to the stretched exponential model.

Composition (ERE:EPE)	***G* (Pa)**	***G*$_e$ (Pa)**	τ_{KWW} **(s)**	$\langle\tau\rangle$ **(s)**	***β***
75:25	1480 ± 404	5188 ± 192	13.9 ± 3.7	49.3 ± 38.8	0.480 ± 0.179
50:50	2633 ± 291	6056 ± 1105	25.0 ± 2.5	47.8 ± 14.3	0.532 ± 0.074
25:75	4312 ± 155	6840 ± 349	35.3 ± 4.0	63.2 ± 8.3	0.534 ± 0.014
0:100	8171 ± 343	6020 ± 848	27.7 ± 4.4	47.4 ± 7.5	0.551 ± 0.011

Table III-2. Stretched exponential (KWW) parameters for stress relaxation experiments with ERE:EPE hydrogels. The experimental data were fit to Eq. III-5 to obtain the parameters (G_e, G, τ_{KWW}, and β). These parameters were used to generate the dashed curves in Figure III-8 a and to evaluate the plateau values of $G(t)$ shown in Figure III-8 b.

4.6 Calculation of the Average Molecular Weight between Cross-links by Theories of Rubber Elasticity (Affine Approximation and Phantom Network Approximation)

For each gel preparation, an average molecular weight between cross-links (M_c) was computed from the high frequency storage modulus and the swelling ratio using rubber elasticity theory. Assuming affine deformation of chains between chemical and physical cross-links, the shear modulus (G) for a network cross-linked in the presence of solvent is given by Eq. III-7 [17, 20].

$$G_{affine} = RT \frac{C_0}{M_C} \left(\frac{\varphi}{\varphi_0} \right)^{1/3} \qquad \text{(Equation III-7)}$$

where R is the gas constant, T is the temperature, C_0 is the initial (preparation state), and φ_0 and φ are the initial (preparation state) polymer volume fraction and equilibrium swollen polymer volume fraction, respectively. To capture the effect of both the chemical and physical cross-links, the shear modulus is taken as the high frequency plateau in the storage modulus, $G'(\infty)$ 'The swollen polymer volume fractions were determined from the mass swelling ratio, Q_m, assuming a gel density of 1 g cm^{-3} (ie. mostly water) and a dry polymer density weighted by the mass fraction of protein and PEG-4VS (approximately 0.8 and 0.2, respectively). The density of the artificial proteins is taken to be that of elastin, 1.3 g cm^{-3} [21], and the density of 10,000 g mol^{-1} PEG is 1.2 g cm^{-3} [22], giving an estimated dry polymer density of 1.28 g cm^{-3}. The dry polymer mass following lyophilization was divided by the cross-linking volume (40 μL) to estimate the initial polymer volume fraction and the initial concentration of polymer in the network before swelling. The values of M_c computed from Eq. III-7 are given in Table III-3, column 4.

Composition (ERE:EPE)	Q_m	$G'(\infty)$ (kPa)	M_c (kg/mol) (affine)	M_c (kg/mol) (phantom)	M_c (kg/mol) (sequence)
100:0	19.7	4.5	49.6	24.8	23.1
75:25	18.1	6.5	33.8	17.2	20.3
50:50	16.1	8.2	28.4	14.7	17.3
25:75	14.7	10.9	20.9	11.0	14.1
0:100	13.5	13.4	17.3	9.3	10.7

Table III-3. Calculated average molecular weight between cross-links (M_c). The swelling ratios (column 2) and high frequency plateau storage moduli (column 3) were used to compute the average molecular weight between cross-links by the affine approximation (column 4) and the phantom network approximation (column 5). The values are compared to the theoretical molecular weight between cross-links determined from the protein sequences (column 6). With the exception of the covalent ERE network, the theoretical values of M_c fall between the values calculated by the affine and phantom network models.

In the phantom network approximation, the cross-links are not fixed in space as in the affine approximation but instead fluctuate. This decreases the free energy per chain and therefore decreases the modulus. In an ideal network, the phantom network modulus is related to the affine modulus from Eq. III-7 through the cross-linker functionality, f [23].

$$G_{phantom} = \left(1 - \frac{2}{f}\right) G_{affine} \qquad \text{(Equation III-8)}$$

The PEG-4VS cross-linker has a functionality of 4. The physical cross-links have a functionality of 5. The molar ratio of chemical to physical cross-links can be used to calculate an average cross-linker functionality, $\overline{f}$, which varies between $\overline{f}$ = 4.3 for EPE gels and $\overline{f}$ = 4 for ERE gels. In

this case the prefactor in Eq. III-8 becomes 0.53 for EPE gels and 0.5 for ERE gels. Including this adjustment in Eq. III-7 gives M_c based on the phantom network model (Table III-3, column 5), which is approximately one-half of the value from the affine model.

The expected or theoretical molecular weight between cross-links in ideal ERE:EPE gels is based on the protein sequences and the molar ratio of each protein in the gelation mixture. In a fully cross-linked EPE gel, in which all chain ends are linked by PEG-4VS and all P midblocks participate in physical cross-links, the average molecular weight between cross-links is calculated as the average of the molecular weight of the segment N-terminal to the P domain and the segment C-terminal to the P domain. These chains are predominantly elastin-like repeats and PEG. The N- and C-terminal segments of EPE have molecular weights of 8763 Da and 7563 Da, respectively. Each arm of the 4-arm PEG vinyl sulfone has a molecular weight of 10,000/4 = 2500 Da. This gives a theoretical average molecular weight between cross-links of 10,663 Da. In a fully cross-linked ERE gel, the average molecular weight between cross-links is calculated as the molecular weight of the protein between the cysteine residues (18,058 Da) plus two PEG arms (2 x 2500 Da), giving an M_c of 23,058 Da. The theoretical values of M_c for the 75:75, 50:50, and 25:75 ERE:EPE gels, which are calculated from the molar ratio of EPE and ERE in the cross-linking reaction, are listed in Table III-3, column 6.

The calculated values of M_c for the five hydrogel preparations were in reasonable agreement with the theoretical values determined from the protein molar masses. Both the affine and phantom network models have been used previously to describe networks formed by cross-linking PEG macromers [24-26]. In these studies, the experimental data were best modeled by the phantom approximation at lower initial polymer volume fractions and the affine approximation at higher initial polymer volume fractions. With the exception of ERE gels, the theoretical values of

M_c of the gels prepared in this work fall between the values calculated by the affine model and by the phantom network model. In ERE gels, the theoretical value is close to the value calculated by the phantom network model. One possible explanation for this observation is that the covalent cross-links fluctuate as modeled by the phantom approximation whereas the larger physical cross-links do not.

The estimation of M_c described here assumes that a perfect network is formed and that the chains between cross-links behave ideally, which is almost certainly not the case. Non-idealities such as loops, missed cross-links (chemical or physical), dangling chains, and entanglements likely exist in the gels. These effects might explain some of the discrepancies between the theoretical values of M_c and the calculated values of M_c.

4.7 Disrupting Physical Cross-linking by Protein Denaturation

The role of protein folding and protein-protein interactions in mediating physical cross-linking was investigated by characterizing the rheological behavior of PEP and EPE hydrogels in buffer containing the protein denaturant urea. As shown in Figure III-9 a and b, PEP gels prepared in solutions that contain up to 1.5 M urea maintain high frequency elastic behavior. A gel-sol transition occurs at a urea concentration of 1.75 M, as indicated by the arrow in Figure III-9 c where $G' = G''$ at 100 rad s^{-1}. In contrast to PEP, EPE cross-linked with PEG-4VS can be swollen in buffer containing 8 M urea without dissolving the network. Under these conditions, however, the frequency-dependence of G' and the maximum in G'' are abolished (Figure III-9 d), and EPE gels closely resemble ERE gels. This again suggests that P domains in neighboring EPE chains associate noncovalently and that this association can be disrupted under denaturing conditions. By

exploiting these phenomena, one can design protein hydrogels that switch between elastic and viscoelastic behavior in response to environmental cues.

4.8 Disupting Physical Cross-linking by Mutation of the P Domain

To define more fully the role of protein sequence in determining bulk hydrogel properties, the effect of a point mutation in the P domain that is expected to disrupt noncovalent chain association was assessed. Gunasekar *et al*. identified aliphatic residues along the hydrophobic face of the COMP coiled-coil domain that are required for maintaining its structure and oligomerization state [27]. Most notably, a single leucine-to-alanine point mutation at position 44 (Figure III-1 a, denoted by *) results in both decreased helicity (16.6% versus 70.1% for the wild-type P domain) and reduced pentamerization [27]. An EPE variant containing this point mutation (denoted EPE L44A) was prepared (Figures III-2, III-3, and III-4), and hydrogels were formed by covalent cross-linking with PEG-4VS. The modified P domains in EPE L44A are expected to be largely unfolded and incapable of forming physical cross-links. Consistent with this view, hydrogels prepared from EPE L44A do not exhibit the high and low frequency plateau storage moduli characteristic of hydrogels containing EPE (Figure III-10). Instead, *G'* is nearly frequency-independent over the experimental range of 0.001-100 rad s^{-1}, demonstrating that a single mutation is sufficient to abolish physical cross-linking. Because the wild-type and mutant P domains differ by only a single amino acid, the physical cross-linking observed in EPE hydrogels can be attributed to highly specific interactions among folded P domains rather than nonspecific aggregation though hydrophobic or electrostatic interactions, as these interactions would likely also be present between mutant P domains.

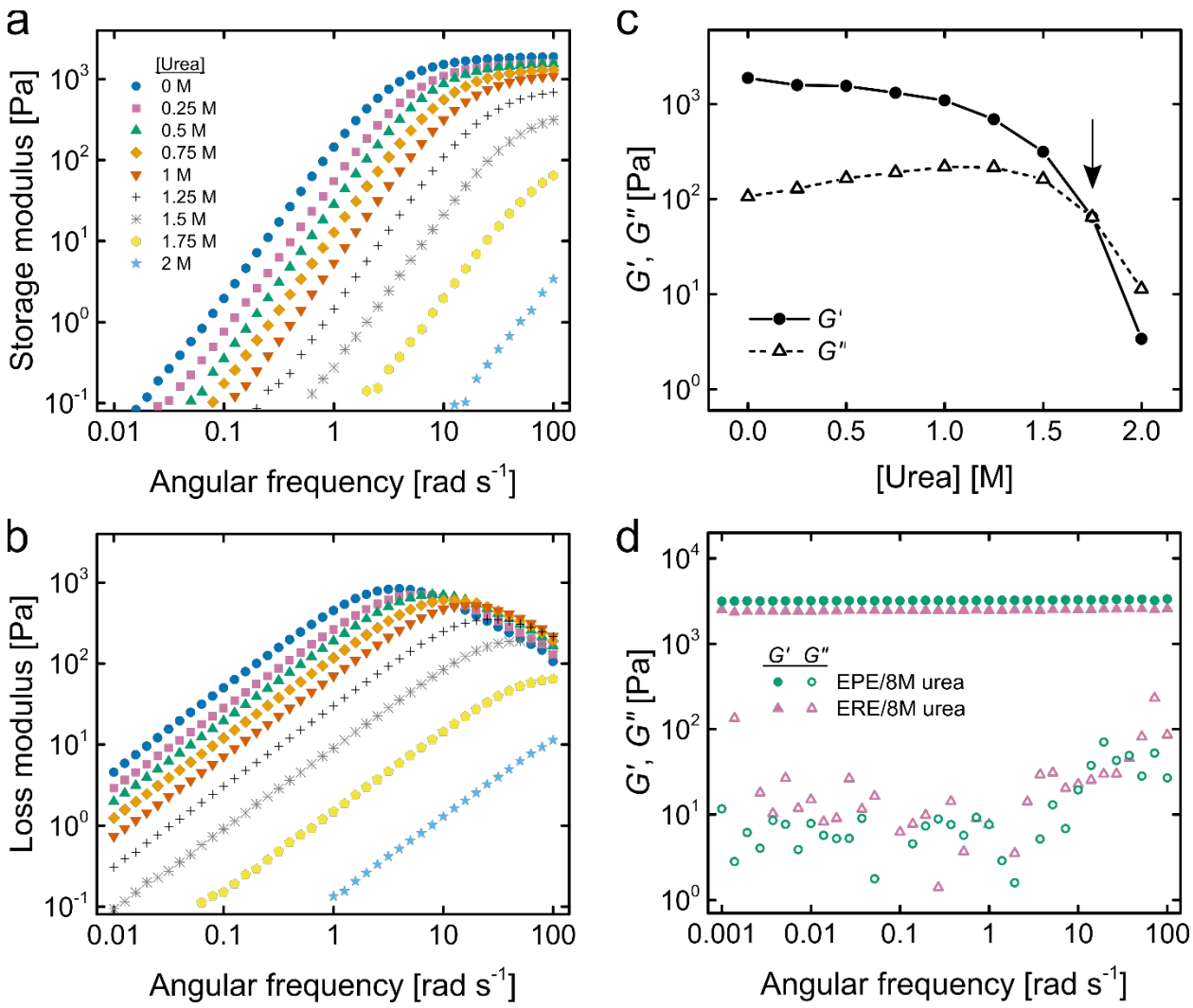

Figure III-9. Disruption of physical cross-linking by denaturant. Storage moduli (**a**) and loss moduli (**b**) of 7 wt% PEP prepared in increasing concentrations of urea at 25 °C, 10% strain amplitude. (**c**) The high frequency values of *G'* and *G"* (at 100 rad s^{-1}) show a decrease in elasticity associated with a loss of physical cross-linking at increasing urea concentrations. An arrow marks the urea concentration of 1.75 M where *G'* and *G"* are equal at 100 rad s^{-1}. (**d**) When EPE and ERE gels are swollen in buffer containing 8 M urea, *G'* is independent of the oscillation frequency and *G"* does not exhibit a maximum (25 °C, 1% strain amplitude). The mass swelling ratios for EPE and ERE swollen in PBS/8 M urea are 32.3 and 34.7, respectively.

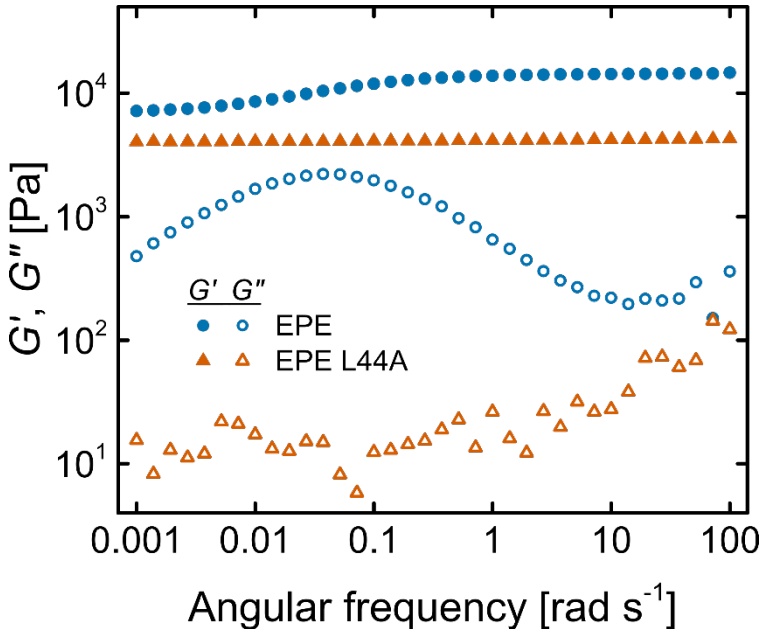

Figure III-10. Disruption of physical cross-linking by a point mutation within the P domain. Hydrogels prepared from the EPE variant EPE L44A (orange triangles) exhibit elastic behavior characterized by a frequency-independent *G'* (filled symbols) and a small loss modulus (open symbols). The frequency sweep of an EPE gel swollen in PBS (blue circles) is shown for comparison. The mass swelling ratio of EPE L44A gels in PBS is 21.7, similar to ERE gels.

5. Conclusions

Previously, chemical cross-links have been introduced into physical gels prepared from zwitterionic polymers, gelatin, and artificial proteins to stabilize these fragile materials against thermal or mechanical disruption [28-31]. Here, dynamic physical cross-links were incorporated into covalent hydrogel networks using engineered protein domains in order to program the time-dependent response to material deformation. Combining covalent and noncovalent cross-linking in gels is emerging as a promising strategy for improving material toughness and resistance to fracture, and mechanical unzipping of coiled-coil domains or analogous processes of programmed

energy dissipation might lead to similar improvements in gel toughness [32-35]. Transient physical cross-linking also has important implications for biological networks, as shown (for example) by the frequency-dependent dynamic moduli of actin networks cross-linked with α-actinin or heavy meromyosin [36, 37]. Stress relaxation and energy dissipation in these networks have been attributed to reversible association of actin cross-links, analogous to the association of the engineered P domains described in this work. In addition to the intracellular cytoskeletal network, the viscoelasticity of the extracellular environment is also an important regulator of cellular behavior on two-dimensional substrates and within three-dimensional matrices [38, 39]. The capacity to program chain sequence at the genetic level opens important new opportunities in the exploration of macromolecular behavior in both biological and engineered systems.

6. References

[1] J.-F. Lutz, M. Ouchi, D.R. Liu, M. Sawamoto *Science* **2013** *341*, 1238149.

[2] K.A. Dill, J.L. MacCallum *Science* **2012** *338*, 1042.

[3] B.V. Slaughter, S.S. Khurshid, O.Z. Fisher, A. Khademhosseini, and N.A. Peppas *Adv. Mater.* **2009** *21*, 3307.

[4] M.W. Tibbitt, K.S. Anseth *Biotechnol. Bioeng.* **2009** *103*, 655.

[5] S.C. Rizzi, J.A. Hubbell *Biomacromolecules* **2005** *6*.

[6] R.A. McMillan, V.P. Conticello *Macromolecules* **2000** *33*.

[7] W.A. Petka, J.L. Harden, K.P. McGrath, D. Wirtz, and D.A. Tirrell *Science* **1998** *281*.

[8] P.J. Skrzeszewska, F.A. de Wolf, M.W.T. Werten, A.P.H.A. Moers, M.A. Cohen Stuart, and J. van der Gucht *Soft Matter* **2009** *5*, 2057.

[9] W. Shen, K. Zhang, J.A. Kornfield, D.A. Tirrell *Nat. Mater.* **2006** *5*.

[10] T.K.L. Meyvis, S.C. De Smedt, J. Demeester, W.E. Hennink *J. Rheol.* **1999** *43*, 933.

[11] D.W. Urry *J. Phys. Chem. B* **1997** *101*, 11007.

[12] V.N. Malashkevich, R.A. Kammerer, V.P. Efimov, T. Schulthess, and J. Engel *Science* **1996** *274*, 761.

[13] A.L. Main, T.S. Harvey, M. Baron, J. Boyd, and I.D. Campbell *Cell* **1992** *71*, 671.

[14] D.T. McPherson, J. Xu, D.W. Urry *Protein Expression Purif.* **1996** *7*, 51.

[15] B.D. Olsen, J.A. Kornfield, D.A. Tirrell *Macromolecules* **2010** *43*.

[16] S. Tang, M.J. Glassman, S. Li, S. Socrate, and B.D. Olsen *Macromolecules* **2014** *47*, 791.

[17] M.P. Lutolf, J.A. Hubbell *Biomacromolecules* **2003** *4*, 713.

[18] J.D. Ferry, *Viscoelastic Properties of Polymers* 3rd ed. Wiley, New York **1980**.

[19] J.W. Goodwin, R.W. Hughes, *Rheology for Chemists: An Introduction* 2nd ed. RSC Publishing, Cambridge **2008**.

[20] N.A. Peppas, E.W. Merrill *J. Appl. Polym. Sci.* **1977** *21*, 1763.

[21] M.A. Lillie, J.M. Gosline *Biopolymers* **2002** *64*, 115.

[22] 2012. *Polyethylene glycol [MAK Value Documentation, 1998]*. *The MAK-Collection for Occupational Health and Safety.* 274-270.

[23] M. Rubinstein, R.H. Colby, *Polymer Physics* Oxford Univ. Press, New York **2003**.

[24] Y. Gnanou, G. Hild, P. Rempp *Macromolecules* **1987** *20*, 1662.

[25] Y. Akagi, J.P. Gong, U.-i. Chung, T. Sakai *Macromolecules* **2013** *46*, 1035.

[26] Y. Akagi, T. Katashima, Y. Katsumoto, K. Fujii, T. Matsunaga, U.-i. Chung, M. Shibayama, and T. Sakai *Macromolecules* **2011** *44*, 5817.

[27] S.K. Gunasekar, M. Asnani, C. Limbad, J.S. Haghpanah, W. Hom, H. Barra, S. Nanda, M. Lu, and J.K. Montclare *Biochemistry* **2009** *48*, 8559.

[28] F. Bode, M.A. da Silva, A.F. Drake, S.B. Ross-Murphy, and C.A. Dreiss *Biomacromolecules* **2011** *12*, 3741.

[29] Z. Zhang, T. Chao, S. Jiang *J. Phys. Chem. B* **2008** *112*, 5327.

[30] R.E. Sallach, W. Cui, J. Wen, A. Martinez, V.P. Conticello, and E.L. Chaikof *Biomaterials* **2009** *30*.

[31] W. Shen, R.G.H. Lammertink, J.K. Sakata, J.A. Kornfield, and D.A. Tirrell *Macromolecules* **2005** *38*.

[32] J.-Y. Sun, X. Zhao, W.R.K. Illeperuma, O. Chaudhuri, K.H. Oh, D.J. Mooney, J.J. Vlassak, and Z. Suo *Nature* **2012** *489*, 133.

[33] Z.S. Kean, J.L. Hawk, S. Lin, X. Zhao, R.P. Sijbesma, and S.L. Craig *Adv. Mater.* **2014** *26*, 6013.

[34] J.A. Neal, D. Mozhdehi, Z. Guan *J. Am. Chem. Soc.* **2015** *137*, 4846.

[35] X. Zhao *Soft Matter* **2014** *10*, 672.

[36] S.M.V. Ward, A. Weins, M.R. Pollak, D.A. Weitz *Biophys. J.* **2008** *95*, 4915.

[37] O. Lieleg, M.M.A.E. Claessens, Y. Luan, A.R. Bausch *Phys. Rev. Lett.* **2008** *101*, 108101.

[38] O. Chaudhuri, L. Gu, M. Darnell, D. Klumpers, S.A. Bencherif, J.C. Weaver, N. Huebsch, and D.J. Mooney *Nat. Commun.* **2015** *6*, 6365.

[39] D.D. McKinnon, D.W. Domaille, T.E. Brown, K.A. Kyburz, E. Kiyotake, J.N. Cha, and K.S. Anseth *Soft Matter* **2014** *10*, 9230.